Publishing House
AKAPIT

COMPUTER METHODS IN MATERIALS SCIENCE

Informatyka w Technologii Materiałów

Vol. 11, 2011, No. 1

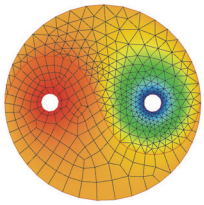

PARTICLE DISTANCE DISTRIBUTIONS AND THEIR EFFECT ON PRECIPITATION STRENGTHENING

BERNHARD SONDEREGGER[1, 2*], IVAN HOLZER[1], ERNST KOZESCHNIK[3], CHRISTOF SOMMITSCH[1]

[1] Institute for Materials Science and Welding, Christian Doppler Laboratory for Materials Modelling and Simulation, Graz University of Technology, Kopernikusgasse 24, 8010 Graz, Austria
[2] Materials Center Leoben Forschung GmbH, Rosseggerstraße 12, 8700 Leoben, Austria
[3] Christian Doppler Laboratory for Early Stages of Precipitation, Institute of Materials Science and Technology, Vienna University of Technology, Favoritenstraße 9-11/ E308, 1040 Vienna, Austria
**Corresponding author: bernhard.sonderegger@tugraz.at*

Abstract

In this work, a general formulation of particle distances in glide planes is derived for arbitrary size distributions. The approach is designed to use the results of Wagner-Kampmann-type models. Size distributions are represented by a set of precipitate classes, where each class contains precipitates of a specific radius and a corresponding number density. The outputs of the calculation are not only particle distances, but particle distance distributions. This representation provides the convenience that any user-defined criterion for the precipitate-dislocation interaction can be applied; e.g. the side condition that at least one third of all spaces between obstacles have to be "open" for dislocation movement in order to allow plastic deformation. As a result, the combination of distribution function and side condition allows a direct calculation of the precipitates strengthening effect. It is shown, that the accordance of simulation and measurements is very promising. The method thus provides the potential to bridge the gap between the simulation of precipitate parameters and the quantitative calculation of precipitate strengthening.

Key words: : precipitate distances, precipitation hardening

1. INTRODUCTION

In a wide range of materials, precipitation hardening is one of the key mechanisms for strengthening, e.g. for enhancing the yield stress or increasing the creep strength. Basically, a high number of precipitates block dislocation movements and thus hinder plastic deformation. The essential parameter in the assessment of the threshold stresses is the particle distance in glide planes. Despite the importance of this parameter, only very basic equations for its calculation can be found in literature, which are generally adopting phase fractions and mean particle sizes as input parameters. These simple approaches may work in some cases, but are generally prone to systematic deviations as soon as the size distributions get broad or multimodal.

The first works on this topic are based on general statistical considerations of Chandrasekhar (1943) and completed by Fullman (1953). In these works, the mean distance of next-nearest neighbor pairs is calculated with the assumption of random particle distributions. Furthermore, all particles are assumed to be spherical and of the same size. Despite the spatial extension of the precipitates, their centers can approach arbitrarily close. Fullmans result for center-to-center particle distances in glide planes is given in equation (1):

ISSN 1641-8581

$$\lambda_{2D,CC} = C \cdot rf^{-1/2} \qquad (1)$$

where $\lambda_{2D,CC}$ is the mean distance between the particle centers in the glide plane, r is the mean radius, f the phase fraction and C a constant with C=0.7236. Other authors assume simpler configurations such as quadratic arrangements of the precipitates, which lead to a different constant in equation 1, C=0.8862 (Lui & Le May, 1975; Nembach, 1982).

Kocks (1966a) reviews a number of different assumptions for the spatial distribution of the precipitates and provides the according correction factors relative to the random distribution geometry. The result of Fullman and the variations collected by Kocks are exact for zero phase fractions and equally-sized precipitates. The latest improvement was introduced by Leggoe (2005), who computed correction factors for equally-sized precipitates numerically, up to phase fractions of most densely packed structures. This work considers the increased ordering of the precipitate arrangements at high phase fractions.

Some works criticize the missing physical significance of the nearest neighbor distance and introduce a different definition of precipitate distances, instead. Russell and Brown (1972) defined the corresponding 'Friedel spacing' as the effective spacing of weak obstacles along a slightly bowed dislocation line. Their expression of λ is identical to equation (1) with a constant of C = 1.7724, or, in a slightly revised model of Brown (1975), C = 1.4472. Because Russel and Brown derived only center-to-center distances, P. M. Kelly (1973) introduced a simple modification for surface-to-surface distances, which reads

$$\lambda_{2D,SS} = C \cdot rf^{-1/2} - \frac{\pi}{2} r \qquad (2)$$

Again, all constants have been derived under the assumption of small phase fractions, and the center of precipitation can approach arbitrarily close.

Nevertheless, the nearest-neighbor distance can conveniently be applied to the calculation of precipitation hardening, if a slight modification is introduced. As Ashby (1968) pointed out, each spacing between a pair of particles has its own passing stress. Additionally, it was shown by Kocks (1966a; 1966b) that extensive slip can first occur at the critical value of the applied stress, such that about one third of the spacings between the particles are "transparent". In other words, one third of the nearest neighbor distances have to exceed a critical value λ. This criterion is going to be used in the further course of this work.

2. NEAREST NEIGHBOR DISTANCES OF PRECIPITATES WITH ARBITRARY SIZE DISTRIBUTIONS

In this section, the calculation of the critical distance λ is described. The first step is the derivation of a probability distribution for nearest neighbor distances. Second, the criterion of Kocks (1966a; 1966b) is applied to find the critical distance. Side conditions are random distribution of the precipitates and arbitrary size distributions, which are represented by size classes. Contrary to the works cited before, particle centers must keep a minimum distance to avoid overlap.

Assume a glide plane with an intersecting precipitate. The center of the precipitate is not necessarily within the glide plane. The projected radius of the particle in the plane is given by r_A. Assume a second precipitate with the surface to surface distance λ_{SS}. The closest possible center-to-center distance of this particle in the plane is thus $2r_A$, as sketched in figure 1. The center of this precipitate lies within the infinitesimal area dA. To make sure the particle is the next neighbor, the area A must be empty.

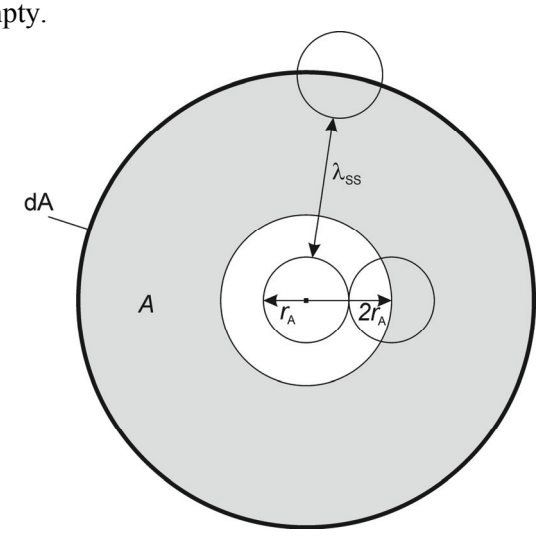

Fig. 1. *Precipitate and its next nearest neighbor in a glide plane.*

When the number density of particles in the glide plane is given by n_A, the number of particles dn in the area dA can be calculated as:

$$dn = n_A \cdot dA \qquad (3)$$

To include the condition '*A is free of particles*', we introduce w_A as the probability of at least one particle placed within A. We can then calculate the probability density of the nearest neighbor placed

within dA, having the surface-to-surface distance λ_{SS}:

$$dW = (1 - w_A) \cdot (n_A \cdot dA) \tag{4}$$

The number of particles per unit area, n_A, can be easily calculated by a summation of all particles intersecting the glide plane. We introduce i size classes, denote the according radii with r_i and the number densities in the volume with $n_{V,i}$:

$$n_A = \sum_i n_{V,i} \cdot 2r_i \tag{5}$$

Furthermore, the area A can be split into η very small pieces. When there is no precipitate in A, there is also no precipitate in any of the sub-areas. If these areas are infinitesimally small, the probability of a particle to be in one of the areas becomes

$$w_\eta = n_A \cdot \frac{A}{\eta} \tag{6}$$

and w_A can be calculated as

$$(1 - w_A) = \lim_{\eta \to \infty} (1 - w_\eta)^\eta = \exp\left(-2A \sum_i n_{V,i} r_i \right) \tag{7}$$

The probability density dW is thus given by

$$dW = \exp\left(-2A \cdot \sum_i n_{V,i} r_i \right) \cdot \left(2 \sum_i n_{V,i} r_i \cdot dA \right) \tag{8}$$

With an area A of

$$A = (\lambda_{SS} + 2r_A)^2 \pi - (2r_A)^2 \pi \tag{9}$$

Using equation (9), equation (8) can be transformed and dW expressed depending on dλ_{SS}:

$$dW = \exp\left(-2\left[(\lambda_{SS} + 2r_A)^2 \pi - (2r_A)^2 \pi \right] \cdot \sum_i n_{V,i} r_i \right) \cdot \left(4\pi (\lambda_{SS} + 2r_A) \sum_i n_{V,i} r_i \cdot d\lambda_{SS} \right) \tag{10}$$

with the solution

$$W = 1 - \exp\left(-2\pi \left[(\lambda_{SS} + 2r_A)^2 - (2r_A)^2 \right] \cdot \sum_i n_{V,i} r_i \right) \tag{11}$$

W depicts the probability, that a nearest neighbour distance is smaller than λ_{SS}. If we introduce the criterion of Kocks, we can set $W = 2/3$ and finally get

$$\lambda_{SS} = \sqrt{\frac{\ln(3)}{2\pi \sum_i n_{V,i} r_i} + (2r_A)^2} - 2r_A \tag{12}$$

The mean projected radius r_A can be calculated as mean value of all projected radii, weighted by the probability that the corresponding precipitates intersect the glide plane, which leads to:

$$r_A = \sqrt{\frac{2}{3}} \cdot \frac{\sum_i n_{V,i} \cdot r_i^2}{\sum_i n_{V,i} \cdot r_i} \tag{13}$$

For comparison, equation (12) can be reduced to systems with equally-sized precipitates:

$$\lambda_{SS} = \sqrt{\frac{\ln(3)}{2\pi n_V r} + \frac{8}{3} r^2} - \sqrt{\frac{8}{3}} \cdot r \tag{14}$$

3. COMPARISON WITH NUMERICAL SIMULATION

In this section, a numerical simulation is set up with the software package MatLab ®. The simulation is fed by various size distributions with phase fractions reaching from 0.5 up to 40%. In each case, 10^5 precipitates were placed randomly in a volume and cut by a glide plane. The size distributions were represented by 100 size classes. After the calculating the distance distributions, $\lambda_{SS,num}$ was defined as the critical spacing according to the criterion of Kocks (1966a; 1966b). Then, equation (12), the simplified version equation (14) and the classical solution of Fullman (1953) are tested against the numerical simulation. For completion, the effective Friedel length (Kelly, 1973, Russel and Brown, 1972) is added to the comparison. Three cases were tested:

Case a: 24 lognormal distributions. r_{mean} constant, r_{median} varies from $0.04r_{mean}$ to $0.96r_{mean}$, f = 2%. Small median radii depict very broad, high median radii narrow size distributions.

Case b: 20 bimodal distributions of two Gauss-peaks. Both peaks contain the same number of particles. $r_{2,mean} = 5r_{1,mean}$. The standard deviation σ is varied from $0.05r_{mean}$ to r_{mean}. f = 2%. Small σ represented separated peaks, with high σ the peaks are overlapping.

Case c: 80 lognormal distributions. r_{mean} constant, r_{median} constant at $0.4r_{mean}$. f varies from 0.5% to 40%.

With cases a) and b), the impact of size distributions at low phase fractions is tested, with case c), the impact of high phase fractions is tested in com-

bination with a broad size distribution. Figures 2 and 3 show the deviation of each method from the exact numerical simulation.

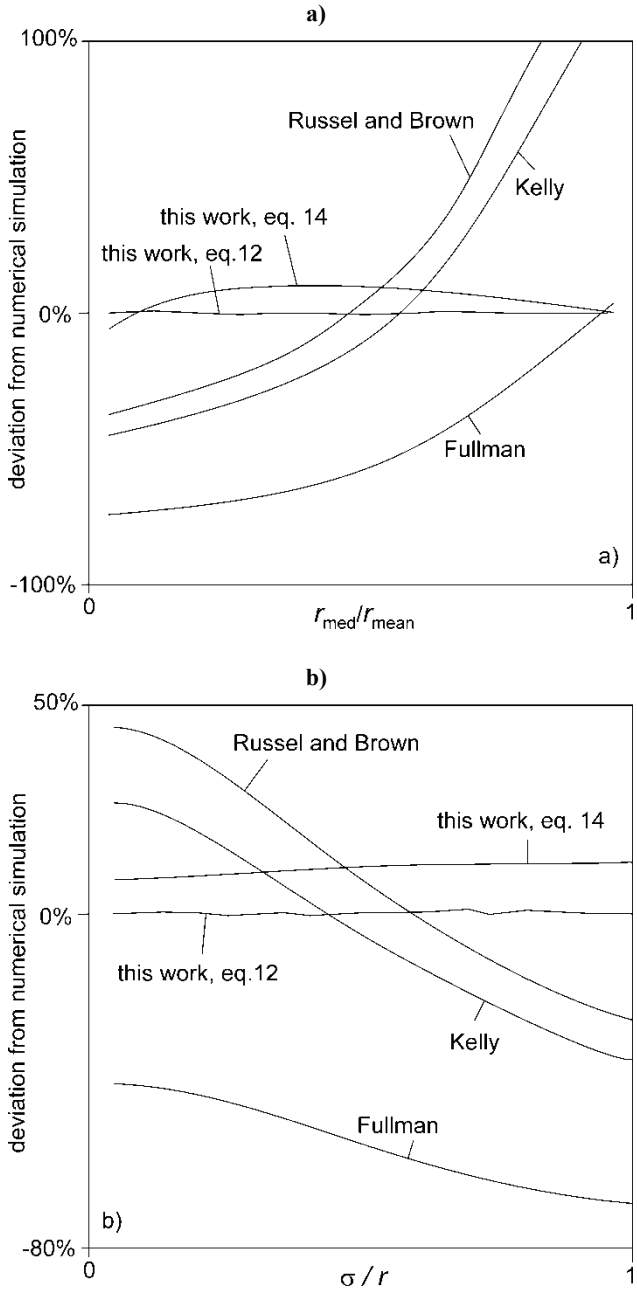

Fig. 2. *Deviation of the methods from the numerical result. Case a) Lognormal distributions, Case b) two Gauss peaks.*

From the figures 2a and 2b, it can clearly be seen that the proposed model (equation (12)) is very close to the numerical result for every size distribution, the deviation is smaller than 0.3% in every case. Insignificant scattering is caused by the limited number of precipitates in the simulation. The deviation of the simplified equation (14) stays below 10% in case a) and 13% in case b). In contrast, the methods of Fullman (1953), Russell and Brown (1972) and Kelly (1973) show strong dependence on the width and shape of the size distributions; the difference to the numerical result varies from -75% to +150%. It shall be noted that the result of Fullman is close to ours for narrow size distributions.

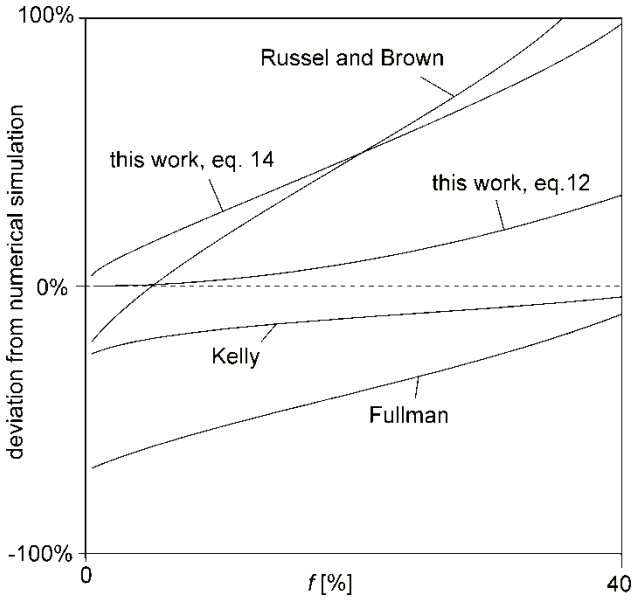

Fig. 3. *Case c), variation of phase fraction.*

In figure 3, the effect of high phase fractions is tested. The predicted precipitate distances of our model tend to overestimate the real distances as soon as the phase fractions become high. However, it remains the most exact method for fractions up to 20%. For higher phase fractions, the method of Kelly (1973) approaches the numerical result. This behavior may be coincidental, since only one size distribution was tested. Because our method showed no dependence on specific size distributions, absolute correction factors for high phase fractions can be taken from this simulation: equation (12) overestimates the real distances by 3.6% (f = 10%), 10% (f = 20%), 20% (f = 30%) and 34% (f = 40%). As pointed out by Leggoe (2005), the reason for this deviation is the increased ordering in the precipitates' positions at higher phase fractions, which is not considered in our model.

5. APPLICATION

In this section, the calculation of precipitate distances is applied to an Fe-1.4at%Cu system, which was aged at 500°C after solution treatment. The according simulation is performed with the software tool MatCalc (Svoboda et. al, 2004; Kozeschnik et. al., 2004) and applies precipitate/matrix interfacial energies calculated by Sonderegger and Kozeschnik (2009a; 2009b; 2010). The simulation considers 500 size classes of fcc and bcc Cu precipitates respectively. Details on the simulations are indicated by

Holzer and Kozeschnik (2010). It shall be emphasized that no fit parameters have been used in the course of the simulation.

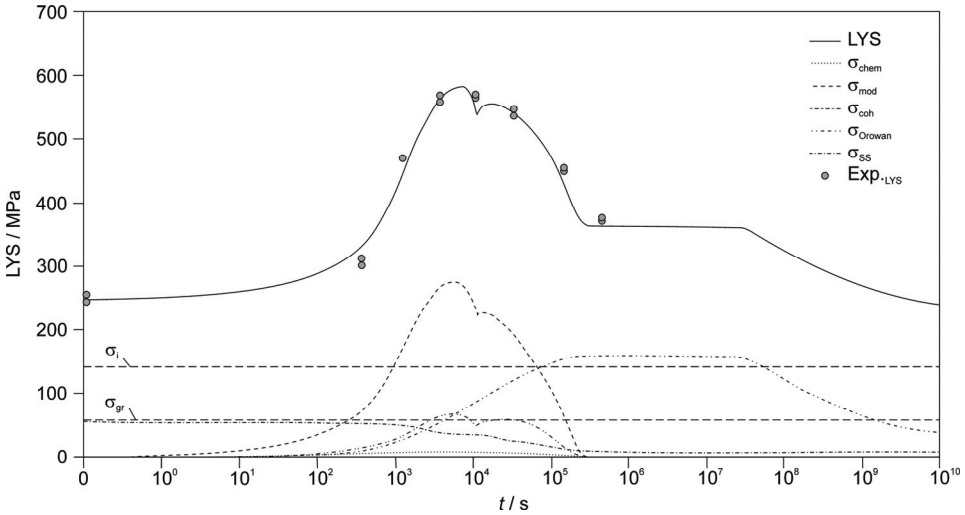

Fig. 4. *Comparison of measured and calculated lower yield strengths (LYS).*

The simulated precipitate parameters are used to compute λ via equation (14), which acts as basis for the calculation of the lower yield stress (LYS). Two groups of strengthening effects are considered: particle independent effects (inherent lattice strength σ_0, grain size strengthening σ_{gr} and solid solution strengthening σ_{ss}) as well as precipitate strengthening (chemical strengthening σ_{chem}, misfit strengthening σ_{coh}, modulus strengthening effect σ_{mod} and strengthening effect of impenetrable particles σ_{Orowan}) (Holzer and Kozeschnik, 2010). Within these effects, σ_{chem}, σ_{mod}, σ_{coh} and σ_{Orowan} are heavily dependent on λ. Generally, the impact of λ on these strengthening effect can be expressed as

$$\tau = C \cdot \frac{Gb}{\lambda} \ln\left(\frac{r_a}{r_i}\right) \cdot f(\Theta_{crit}) \qquad (15)$$

where τ is the strength contribution, C a constant depicting the specific interaction mechanism, G the shear module, b the burgers vector, r_i and r_a the inner and outer cutoff radii of the dislocations and Θ_{crit} the critical bow-out angle of dislocations. All results are compared to measured LYS of Goodman and Brenner (1973). Figure 4 presents the comparison of the measured and calculated LYS, where calculated and measured LYS coincide with excellent agreement.

6. SUMMARY

In this work, a novel analytical approach for the calculation of precipitate distances in dislocation glide planes is presented. The approach is capable of handling arbitrary size distributions and provides very good agreement with numerical simulations. The results can be applied as input parameter for any kind of precipitate strengthening model. The present approach is thus ideal to bridge the gap between precipitate kinetic simulation and the calculation of material properties. On the example of thermal ageing of an Fe-Cu alloy, the model is tested as link between the simulation of precipitate parameters and the calculation of the lower yield strength. In comparison with experimental data, very good agreement could be achieved.

ACKNOWLEDGMENTS

Financial support by the Österreichische Forschungsförderungsgesellschaft mbH, the Province of Styria, the Steirische Wirtschaftsförderungsgesellschaft mbH and the Municipality of Leoben within research activities of the Materials Center Leoben Forschung GmbH under the frame of the Austrian Kplus Competence Center Programme is gratefully acknowledged.

REFERENCES

Ashby, M., 1968, The theory of critical shear stress and work hardening of dispersion-hardened crystals, Metallurgical Society Conference Vol. 47, eds, Ansell, G. S., Cooper, T. D., Lenel, F. V., Gordon and Breach, New York, 143-205.

Brown, L. M., 1975, Comment on the 'Friedel relation' in precipitate hardening, *Scripta Metall.*, 9, 591-593.

Chandrasekhar, S., 1943, Stochastic problems in physics and chemistry, *Rev. Mod. Phys.*, 15, 1-89.

Fullman, R. L., 1953, Measurement of approximately cylindrical particles in opaque samples, *Trans. AIME*, 197, 1267-1268.

Goodman, S. R., Brenner, S. S., Low Jr., J. R., 1973, FIM-atom probe study of precipitation of Copper from Iron-1.4at% Copper, *Metall. Trans*., 4, 2363-2369.

Holzer, I., Kozeschnik, E., 2010, Computer simulation of the yield strength evolution in Cu-precipitation strengthened ferritic steel, *Mater. Sci. Engng*., A 527, 3546-3551.

Kelly, P. M., 1973, The quantitative relationship between microstructure and properties in two-phase alloys, *Int. Met. Rev*., 18, 31-36.

Kocks, U. F., 1966a, On the spacing of dispersed obstacles, *Acta Metall*., 14, 1629-1631.

Kocks, U. F., 1966b, A statistical theory of flow stress and work-hardening, *Phil. Mag*., 13, 541-550.

Kozeschnik, E., Svoboda, J., Fratzl, P., Fischer, F. D., 2004, Modelling of kinetics in multi-component multi-phase systems with spherical precipitates –II: Numerical solution and application, *Mater. Sci. Engng*., A 385, 157-165.

Leggoe, J. W., 2005, Nth- nearest neighbor statistics for analysis of particle distribution data derived by micrographs, *Scripta Mater*., 53, 1263-1268.

Lui, M. W., Le May, I., 1975, On the "Friedel relation" in precipitate hardening, *Scripta Metall*., 9, 587-589.

Nembach, E., 1982, How the choice of the dislocations' outer cut-off radius affects the evaluation of precipitate hardening data", *Scripta Metall*., 16, 1261-1265.

Russell, K. C., Brown, L. M., 1972, Dispersion strengthening model based on differing elastic-moduli applied to Iron-Copper system, *Acta Metall. Mater*., 20, 969-974.

Sonderegger, B., Kozeschnik, E., 2009a, Generalized nearest-neighbor broken-bond analysis of randomly oriented interfaces in multicomponent fcc and bcc structures, *Metall. Mater. Trans*., 40A, 499-510.

Sonderegger, B., Kozeschnik, E., 2009b, Size dependence of the interfacial energy in the generalized nearest-neighbor broken-bond approach, *Scripta Mater*., 60, 635-638.

Sonderegger, B., Kozeschnik, E., 2010, Interfacial energy of diffuse phase boundaries in the generalized broken-bond approach, *Metall. Mater. Trans. 41A*, 3262-3269.

Svoboda, J., Fischer, F. D., Fratzl, P., Kozeschnik, E., 2004, Modelling of kinetics in multi-component multi-phase systems with spherical precipitates –I: Theory, *Mater. Sci. Engng*., A 385, 166-174.

ROZKŁAD ODLEGŁOŚCI MIĘDZY CZĄSTKAMI I ICH WPŁYW NA UMOCNIENIE WYDZIELENIOWE

Streszczenie

W pracy sformułowano metodę oceny odległości pomiędzy cząstkami w płaszczyznach poślizgu dla dowolnego rozmiaru cząstek wydzieleń. Metoda jest przystosowana do wykorzystania wyników z modelu typu Wagnera-Kampmanna. Rozkład wielkości cząstek jest reprezentowany przez zbiór klas wydzieleń, w którym każda klasa zawiera wydzielenia o pewnym specyficznym promieniu i odpowiadającej im gęstości. Wynikiem obliczeń są nie tylko odległości między cząstkami, ale także rozkład tych odległości. Zaletą takich wyników jest możliwość zastosowania dowolnie sformułowanego przez użytkownika kryterium interakcji wydzielenie-dyslokacja, na przykład warunek, że aby możliwe było odkształcenie plastyczne, co najmniej jedna trzecia wszystkich odległości między przeszkodami musi być otwarta dla ruchu dyslokacji. W rezultacie kombinacja funkcji rozkładu odległości i podanego kryterium pozwala na bezpośrednią ocenę umocnienia wydzieleniowego. W artykule wykazano, że symulacje dają wyniki zgodne z obserwacjami doświadczalnymi. Metoda jest zatem krokiem w kierunku wypełnienia luki pomiędzy symulacjami parametrów procesu wydzieleniowego i oceną umocnienia wydzieleniowego.

Received: September 24, 2010
Received in a revised form: November 2, 2010
Accepted: November 17, 2010